



<b>Title</b>	Sub-wavelength infrared imaging of lipids
<b>Authors(s)</b>	Yarrow, Fiona, Kennedy, Eamonn, Salaun, Frederic, Rice, James H.
<b>Publication date</b>	2011-01
<b>Publication information</b>	Yarrow, Fiona, Eamonn Kennedy, Frederic Salaun, and James H. Rice. "Sub-Wavelength Infrared Imaging of Lipids." Optical Society of America, January 2011. <a href="https://doi.org/10.1364/BOE.2.000037">https://doi.org/10.1364/BOE.2.000037</a> .
<b>Publisher</b>	Optical Society of America
<b>Item record/more information</b>	<a href="http://hdl.handle.net/10197/4504">http://hdl.handle.net/10197/4504</a>
<b>Publisher's statement</b>	This paper was published in Biomedical Optics Express and is made available as an electronic reprint with the permission of OSA. The paper can be found at the following URL on the OSA website: <a href="http://www.opticsinfobase.org/boe/abstract.cfm?uri=boe-2-1-37">http://www.opticsinfobase.org/boe/abstract.cfm?uri=boe-2-1-37</a> . Systematic or multiple reproduction or distribution to multiple locations via electronic or other means is prohibited and is subject to penalties under law.
<b>Publisher's version (DOI)</b>	10.1364/BOE.2.000037

Downloaded 2026-05-01 23:47:42

The UCD community has made this article openly available. Please share how this access benefits you. Your story matters! (@ucd\_oa)



© Some rights reserved. For more information

# Sub-wavelength infrared imaging of lipids

Fiona Yarrow, Eamonn Kennedy, Frederic Salaun and James H Rice

NanoPhotonics Research Group, School of Physics, University College Dublin, Belfield,  
Dublin, Ireland  
[James.Rice@UCD.ie](mailto:James.Rice@UCD.ie)

## Abstract:

Infrared absorption spectroscopy of lipid layers was performed by combining optics and scanning probe microscopy. This experimental approach enables sub-diffraction IR imaging with a spatial resolution on the nanometer scale of 1, 2-dioleoyl-*sn*-glycero-3-phosphocholine lipid layers.

© 2010 Optical Society of America

**OCIS codes:** (310.6628) Subwavelength structures, nanostructures; (350.5340) Photothermal effects; (300.6340) Spectroscopy, infrared

---

## References and links

1. J.H. Rice, "Fluorescence microscopy beyond the diffraction limit: Fluorescence microscopy with super-resolution," *Mol. BioSyst.* **3**(11), 781-793, (2007).
2. D. Vobornik, G. Margaritondo, J.S. Sanghera, P. Thielen, I.D. Aggarwal, B. Ivanovc, N.H. Tolk, V. Mannid, S. Grimaldi, A. Lisi, S. Rieti, D.W. Piston, R. Generosi, M. Luce, P. Perfetti, A. Cricenti, "Spectroscopic infrared scanning near-field optical microscopy (IR-SNOM)", *Journal of Alloys and Compounds.* **401**(1-2), 80-85 (2005).
3. M. Brehm, T. Taubner, R. Hillenbrand, F. Keilmann, "Infrared spectroscopic mapping of single nanoparticles and viruses at nanoscale resolution," *Nano Lett.* **6**(7), 1307-1310, (2006).
4. T. R. Albrecht, C.F. Quate, "Atomic resolution with the atomic force microscope on conductors and nonconductors," *Vac. Sci. Technol. A* **6**, 271-275, (1988).
5. A. Huber, A. Ziegler, T. Koeck, R. Hillenbrand, "Infrared nanoscopy of strained semiconductors", *Nature Nanotech.* **4**(3), 153-157 (2009)
6. A. Hammiche, M.H. Pollock, M. Reading, M. Claybourn, P.M. Turner, K. Jewkes, "Photothermal FT-IR spectroscopy: A step towards FT-IR microscopy at a resolution better than the diffraction limit" *Applied Spectroscopy*, **53**(7), 810-815, (1999).
7. A. Hammiche, L. Bozec, M.J. Gorman, J.M. Chalmers, N.J. Everall, G. Poulter, M. Reading, D.B. Grandy, F.L. Martin, H.M. Pollock, "Mid-infrared microspectroscopy of difficult samples using near-field photothermal microspectroscopy," *Spectroscopy*, **19**(2), 20-42, (2004).
8. A. Dazzi, R. Prazeres, F. Glotin, J.M. Ortega, "Analysis of nano-chemical mapping performed by an AFM-based ("AFMIR") acousto-optic technique," *Ultramicroscopy*, **107**(12) 1194-1200, (2007).
9. J. Houel, S. Sauvage, P. Boucaud, A. Dazzi, R. Prazeres, F. Glotin, J.M. Ortega, A. Miard, A. Lemaitre, "Ultraweak-Absorption Microscopy of a Single Semiconductor Quantum Dot in the Midinfrared Range," *Physical Review Letters*, **99**(21), 217404 (1-4), (2007).
10. C. Mayet, A. Dazzi, R. Prazeres, F. Allot, F. Glotin, J.M. Ortega, "Sub-100 nm IR spectromicroscopy of living cells", *Optics Lett.* **33**(14), 1611-1613, (2008).
11. G. Hill, J.H. Rice, S.R. Meech, P. Kuo, K. Vodopyanov, M. Reading, "nano-Infrared surface imaging using an OPO and an AFM", *Optics Letters*, **34**(4), 431-433, (2009).
12. Koynova R and Caffrey M, "An index of lipid phase diagrams" *Chem. Phys. Lipids* **115** 107-219 (2002)
13. Marsh D, *CRC handbook of lipid bilayers* (Boca Raton: CRC Press Inc. USA) (1990)
14. Yeagle P L, *The structure of biological membranes* (Boca Raton: CRC Press USA) (2005)
15. H. T. Jung, "Modelling and recording characteristics of a dye-doped polymer bilayer film" *Applied Physics B*, **70**(2), 237-242, (2000).
16. H.N. Subrahmanyam, S.V. Subramanyam, "Thermal expansion of irradiated polystyrene", *Journal of Materials Science*, **22**(6) 2079-2082, (1987).
17. I.M. Asher, I.W. Levin, "Effects of temperature and molecular interactions on the vibrational infrared spectra of phospholipid vesicles", *Biochimical Biophysical Acta* **468**(1) 63-72 (1977)
18. H.H. Mantsch, A. Martin, D.G. Cameron, "Characterization by infrared spectroscopy of the bilayer to nonbilayer phase transition of phosphatidylethanolamine", *Biochemistry*, **20**(11), 3138-3145, (1981).

---

## 1. Introduction

Absorption spectroscopy is an extensively applied technique for chemical characterisation

that is able to detect both luminescent and non-luminescent materials. It has the potential to yield chemical specific information for virtually all bulk organic samples. A frequently used form of absorption spectroscopy is infrared (IR) absorption spectroscopy. This method measures the absorption of light by materials in the infrared region of the electromagnetic spectrum. The IR energy range spans the resonance frequencies of many common molecular bonds. This enables highly accurate structural elucidation and compound identification of materials using this technique.

However, one of the key limitations of IR absorption spectroscopy is the diffraction limit, which is the primary experimental challenge for well resolved spatial IR imaging [1]. The diffraction limit at c.a.  $\lambda/2$ , results in a resolution of approximately 1  $\mu\text{m}$  when imaging at 3000  $\text{cm}^{-1}$ . Overcoming the diffraction limit is attractive for many areas of research such as nanobiology and semiconductor research, where nanoscale resolution is required in order to fully exploit the potential of these areas.

Near-field IR imaging based on scanning near field optical microscopy (SNOM) has been demonstrated via the use of a customised optical fibre delivery and collection probe [2]. However, this approach is based on the collection of scattered light and consequently provides only indirect access to the IR absorption spectra of materials. This is because the measured signal is a convolution of both the IR absorption and the local dielectric properties of the material studied.

Current alternatives to this method often rely on atomic force microscopy (AFM). AFM measures topographic images of surfaces with very high spatial resolution, i.e. < 10 nm [3]. One example is scattering near-field infrared microscopy (SNIM), which is based on the detection of scattered light from an AFM tip acting as an oscillating antenna [4,5]. This approach has enabled sub-wavelength imaging of heterogeneous surfaces including cells and tissues. However, as with SNOM this approach is a scattering technique, meaning that the IR spectral information recovered does not directly represent IR absorption information.

Direct IR absorption imaging can be achieved using photothermal methods where the AFM cantilever tip acts as an optical excitation detector, while simultaneously recording the image topography [6,7]. Another technique, referred to as AFMIR, has been developed to produce IR imaging and spectroscopy of condensed matter surfaces at resolutions far below the diffraction limit. This method employs excitation radiation tuned to the material IR resonance focused in pulses onto the sample, generating periodic surface oscillations [8]. Propagating acoustic shock fronts from the resonating sample excite different vibration modes of the AFM cantilever [1]. The magnitudes of these modes are then related back to the IR absorption of the sample using Fourier analysis.

AFMIR has been applied to study E. Coli bacteria, epitaxial quantum dots, polymers and live cells [8, 9, 10, 11]. To date, the experimental methodology of AFMIR has predominantly been based on two methods; an attenuated total internal reflection arrangement in combination with IR cyclotron radiation, and a top down configuration using a customised IR laser source. Here, we produce IR spectra and images of individual lipids with a resolution of 37 nm when imaging at a wavelength of 3420 nm (2925  $\text{cm}^{-1}$ ) corresponding to an image resolution of  $\lambda/93$ .

The work presented here demonstrates that AFMIR can be applied to study nano-sized lipid layers. Lipid layers containing a single or limited number of different types of lipids have been studied extensively in biophysical studies to elucidate phase behaviour and packing properties of lipid molecules in a bilayer [12]. Knowledge of the physical properties of these membranes can lead to useful insights about more complex, biological membranes. The choice of 1,2-dioleoyl-*sn*-glycero-3-phosphocholine (DOPC) lipids here is motivated by its abundance in biological systems [13,14].

## 2. Lipid imaging with AFMIR

The bottom-up (b-) AFMIR experimental set-up is shown in Fig 1. IR radiation was generated using an OPO laser (Cohesion) based on a periodically poled LiNbO<sub>3</sub> crystal emitting tuneable IR laser radiation, tuneable over > 3.0 to 3.6 μm. The laser output power was industrially quoted as 2 mW. The laser light was focused onto a 500 μm spot on the sample in order to cover the probed area homogeneously. The excitation energy was set low enough to avoid damaging the sample. An AFM (Veeco Explorer system) was used with a scanner with lateral and vertical scan dimensions of 100 x 100 μm and 10 μm respectively. Silicon nitride tips mounted on a V-shaped cantilever with a nominal spring constant of 0.05 N/m (Veeco) were used.

The AFM was operated in contact mode, with a typical force set-point between 1 and 3 nN. Samples were prepared on standard microscope glass slides. A Stanford SR650 (Sunnyvale, CA, USA) attenuator was used to amplify the signal from the AFM. The signal was routed to the input of an Agilent DSO5012A oscilloscope (Agilent Inc., Santa Clara CA, USA). The scope output was digitally read in using the Agilent connection expert IO libraries suite.

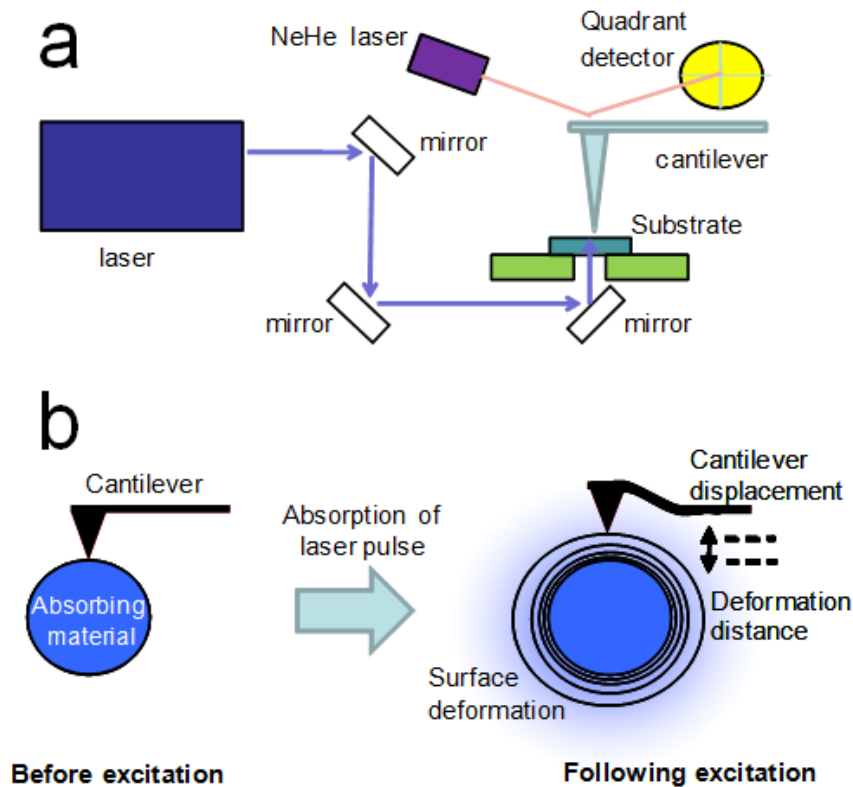


Fig. 1 a) Schematic drawing of the experimental set-up, b) Schematic drawing of origin of the measured signal, before on-resonance excitation, right, the resulting (measured) surface deformation and cantilever displacement

The basis of b-AFMIR comes from optically induced effects that are directly proportional to IR absorption. The AFM cantilever tip was positioned over the sample with the tip in contact with the sample surface (see Fig 1). Following absorption of the incident radiation, the energy absorbed is dissipated through thermal and acoustic mechanisms. Propagating acoustic waves create a deformation in the surface topography which can be detected by the AFM tip. As an IR laser excitation source is tuned into resonance with a vibration mode, absorption of IR radiation increases. The intensity of the deflection maxima for the excited cantilever mode was monitored as a function of excitation wavelength. While the feedback of the AFM counteracted the signal produced by the four quadrants detector, the response time is slower than any deformation induced by the laser burst. Therefore the effect is measured independently of the AFM feedback.

The absorption of the excitation radiation falls exponentially as the light propagates through the absorbing material [15, 16]. The effective spatial resolution is a function of the sample under study, the AFM tip size and the sampling frequency. Previously, AFMIR has been applied to study quantum dots with a spatial resolution of 60 nm [10]. This indicates that the propagation lengths of the acoustic waves that are responsible for the absorption measurement mechanism are short enough in such materials to enable nanoscale imaging.

The IR radiation is directed upward in a novel configuration as shown in Fig. 1 using gold coated mirrors and a lens to direct and focus the laser light. The sample was mounted onto a transparent substrate to facilitate this optical arrangement. Samples were prepared on mica or glass substrates. First, multilamellar vesicles were made by hydrating a dry film of DOPC lipids (1,2-dioleoyl-*sn*-glycero-3-phosphocholine, Avanti Polar Lipid Inc., Alabaster, Alabama, USA) with a 20 mM NaCl (extra pure, Acros Organics) solution in ultrapure water and sonicating for 10 minutes in a bath sonicator (Fisherbrand FB11002, Fisher Scientific, Loughborough, UK) (New 1990). A small amount of the turbid lipid dispersion was then deposited on a freshly cleaved mica or cleaned glass substrate and left to dry overnight under ambient conditions.

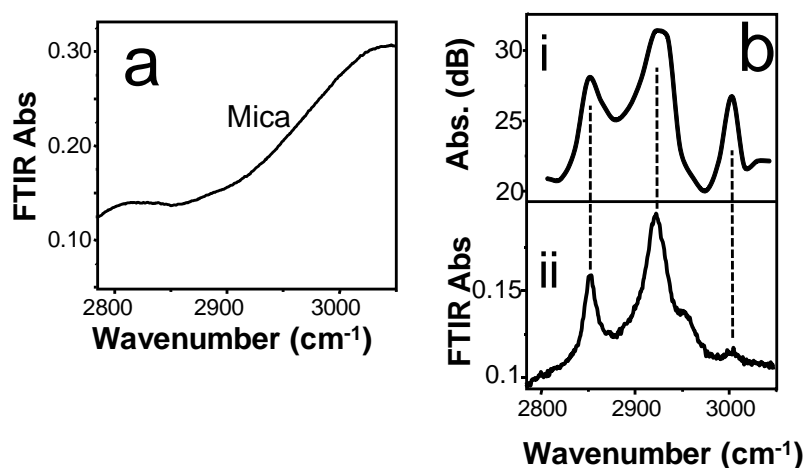


Fig. 2. a) FTIR spectrum of mica, b) IR absorption spectra for lipid, top is the AFMIR spectrum and bottom is the reference FTIR spectrum.

A Fourier Transform IR (FTIR) spectrometer (Varian, model 3100, Palo Alto, CA, USA) was used to record reference IR spectra of the substrate and samples. Measurements of the absorption by the substrate were made. Fig. 2 shows a plot of the variation of the laser wavelength transmitted through the substrate. The FTIR of the mica shows that there is absorption in the IR. A broad band at  $2930\text{ cm}^{-1}$  can be seen along with a small band at  $3030\text{ cm}^{-1}$ . A FTIR spectrum of a film of lipids was recorded and is also shown in Fig 2.b. The spectrum shows large bands at  $2851\text{ cm}^{-1}$ ,  $2925\text{ cm}^{-1}$  and a small band at  $3006\text{ cm}^{-1}$

### 3. Results and discussion

A local IR spectrum was recorded with the AFMIR method. The tip was positioned over a small part of the sample observed in the AFM topography image, with the tip in contact with the sample surface. The cantilever displacement intensity was measured as function of excitation wavelength. This allows reconstruction of the IR spectrum. The intensity of the cantilever oscillation varied on resonance ( $2924\text{ cm}^{-1}$ ) and off resonance ( $2810\text{ cm}^{-1}$ ) with the C-H stretching mode of the lipid's hydrocarbon chains. The intensity of the oscillation of the cantilever as a function of excitation wavelength was recorded.

The resulting AFMIR spectrum of DOPC lipids is shown in Fig 2b. The AFMIR spectrum is shown alongside the FTIR spectrum of DOPC. The two spectra show very similar features. The AFMIR spectrum shown in Fig 2b possesses a wavelength resolution of  $15\text{ cm}^{-1}$ , while the FTIR based spectrum has a wavelength resolution of  $2\text{ cm}^{-1}$ . The bands at  $2851$  and  $2925\text{ cm}^{-1}$  are assigned to symmetric C-H stretching of the methylene groups, respectively [17]. The symmetric and asymmetric C-H stretching of the terminal methyl groups are observed at  $2875$  and  $2956\text{ cm}^{-1}$ . The C-H stretching of the oleoyl chain is observed at  $3006\text{ cm}^{-1}$  [18]. This is in agreement with the position of the peaks observed in the AFMIR spectrum in Fig 2b. There is an increase in the intensity of the band at  $3006\text{ cm}^{-1}$  in the AFMIR spectrum compared to the FTIR spectrum. However, it is noted that the presence of the background from the mica may contribute to the peak intensity in this region, as our spectra indicate mica has a broad FTIR absorption maxima close to the oleoyl chain resonance (Fig. 2a). Other effects may also account for this observed difference in the intensity of the band at  $3006\text{ cm}^{-1}$  in the AFMIR spectrum compared to the FTIR spectrum. This spectral feature difference may arise from the structural form that the localised area of the DOPC lipid is in compared to the average for the bulk material.

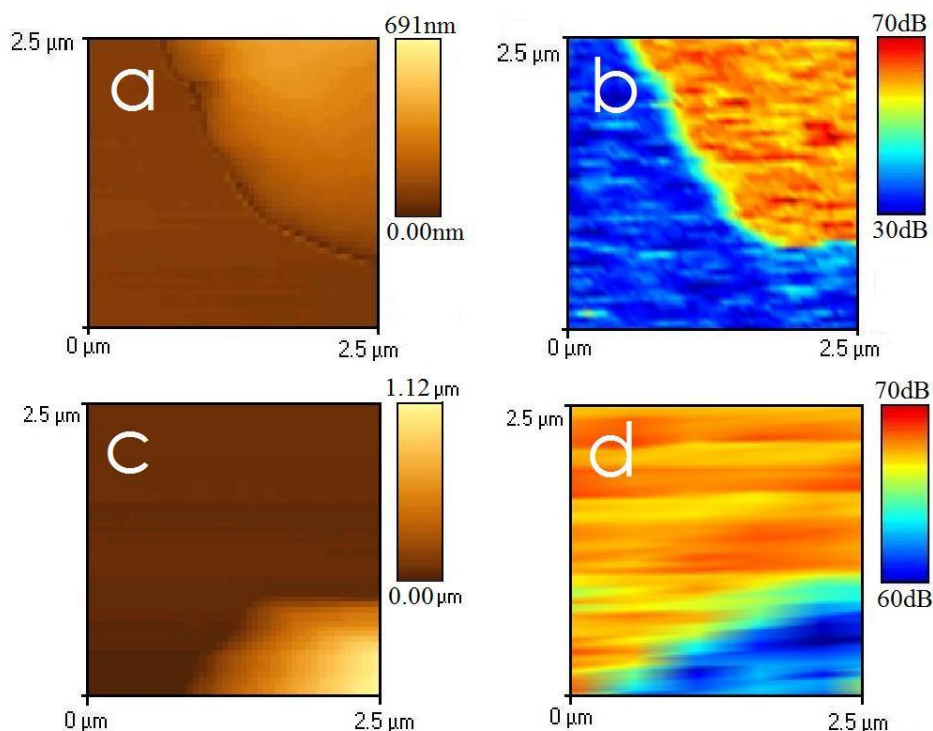


Fig. 3. a) an AFM topography of a lipid section b) the correlating AFMIR scan in relative dB. Distinguishable features are present in both below 100nm. c) A higher lipid and its simultaneous rapid scan AFMIR is presented in d).

AFMIR imaging of a lipid sample was undertaken. Fig. 3a and 3b show a comparison of an AFM topography image with an AFMIR image of a lipid layer recorded with an IR absorption resonance at  $2925\text{ cm}^{-1}$ . This image was created by monitoring the change in intensity of a FFT peak at 390 kHz. Matching surface features are evident when comparing the AFM and AFMIR scans. Additionally, the IR absorption is not fully homogenous throughout the lipid, and shows reduced heating at the sample edges relative to the aggregate's interior. The AFMIR image resolution is defined as  $s/f$  where  $f$  is the FT peak sampling frequency and  $s$  is the AFM scan rate in  $\mu\text{m/s}$ . The resolution has a lower bound imposed by the AFM tip – sample interaction area, which varies with the tip

used. The AFMIR image in Fig. 3a possessed an image resolution of 37 nm. High speed AFMIR was also demonstrated. Fig. 3c and d show a similar comparison of an AFM and AFMIR lipid scan with a reduced lateral resolution of 357 nm. The AFMIR image in Fig 3c was obtained using a temporal accumulation duration of 1.4 seconds per line. A reduction in the higher 450KHz cantilever mode was observed for on sample measurements i.e.  $IR\ Abs \propto dB^{-1}$ . This FT peak was monitored in Fig.3 d). The AFMIR in Fig. 3b has a high signal to noise ratio, enabling a clear distinction between the mica and the lipid layer. The rapid scan seen in Fig. 3d has approximately four times less signal to noise intensity i.e. 10 dB compared to a 40 dB signal range. The reduction in signal to noise occurred because the 450 kHz FT signal has a finite temporal response.

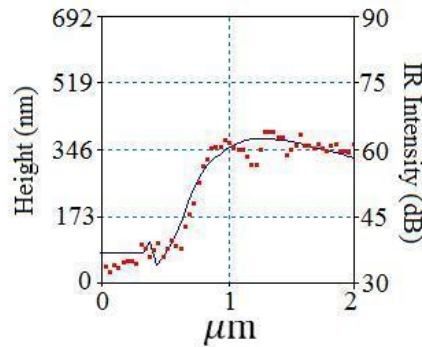


Fig. 4. A lipid side profile showing the AFM topology in black, and a one directional AFMIR scan (red points) with a resolution of 37nm.

A comparison of the AFM topography profile with the AFMIR profile from the image presented in Fig 3a is shown in Fig. 4. The AFMIR follows the AFM topography profile showing the ability of this method to IR image with a high spatial resolution and accuracy. Additionally, as the IR laser was spread homogeneously, specific features of the AFMIR scan reflect the magnitude of its local deformation, which depends on internal chemical structure as well as sample height.

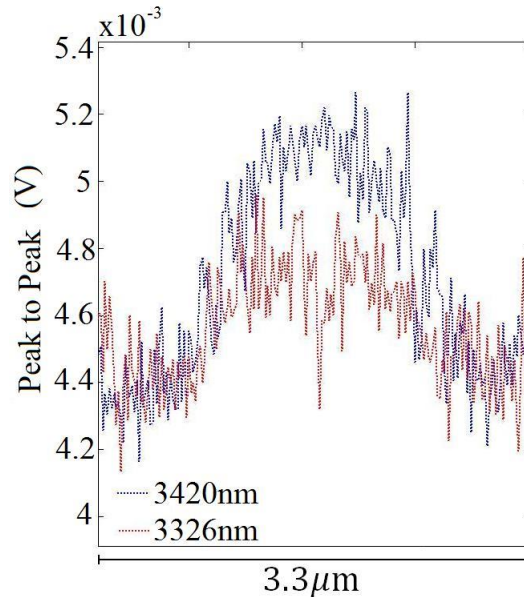


Fig. 5. Cantilever oscillation peak to peak voltages at IR absorption wavelengths tuned to resonance 3420nm (blue) and off of resonance 3326nm (red). A 56% reduction in signal is observed for the off resonance AFMIR.

The effect of changing the laser excitation wavelength was studied. Fig 5 outlines a

profile of AFMIR signal against distance for a particular line scan. The effect of changing the pump laser wavelength from on resonance to an off resonance frequency clearly produces a change in profile intensity. This is illustrated by the cantilever oscillation peak to peak voltages at IR absorption wavelengths tuned to resonance 3420 nm (blue line) and off of resonance 3326 nm (red line). The voltage peak to peak above the 4.4 V background indicates signal reduction of 56% for the off resonance scan when compared to the same lipid at its IR excitation maxima. The intensity observed in the off resonance scan obtained using this method arises from the residual absorption of the lipid at the off resonance wavelength, evident in fig. 2b.

#### **4. Conclusion**

IR absorption spectroscopy of lipid layers was performed using an IR optical parametric oscillator laser and a commercial atomic force microscope. The results show that this experimental approach enables detection and characterization of lipid features. This method of IR spectroscopy can now be applied to study more complex lipid and protein chemical features on the nanoscale.